Available online at www.sciencedirect.com

ScienceDirect

Physics Procedia 67 (2015) 392 – 397

Physics Procedia

25th International Cryogenic Engineering Conference and the International Cryogenic Materials Conference in 2014, ICEC 25–ICMC 2014

Numerical investigation of thermal distribution and pressurization behavior in helium pressurized cryogenic tank by introducing a multi-component model

Wang Lei[a], Li Yanzhong[a,b,*], Liu Zhan[a], Zhu Kang[a]

[a]*Institute of Refrigeration and Cryogenics, Xi'an Jiaotong University, Xi'an,710049,China*
[b]*State Key Laboratory of Technologies in Space Cryogenic Propellants, Beijing,100028, China*

Abstract

An improved CFD model involving a multi-component gas mixture in the ullage is constructed to predict the pressurization behavior of a cryogenic tank considering the existence of pressurizing helium. A temperature difference between the local fluid and its saturation temperature corresponding to the vapor partial pressure is taken as the phase change driving force. As practical application of the model, hydrogen and oxygen tanks with helium pressurization are numerically simulated by using the multi-component gas model. The results present that the improved model produce higher ullage temperature and pressure and lower wall temperature than those without multi-component consideration. The phase change has a slight influence on the pressurization performance due to the small quantities involved.

© 2015 The Authors. Published by Elsevier B.V. This is an open access article under the CC BY-NC-ND license (http://creativecommons.org/licenses/by-nc-nd/4.0/).

Peer-review under responsibility of the organizing committee of ICEC 25-ICMC 2014

Keywords: Cryogenic tank; CFD simulation; Thermal stratification; Heat transfer; Phase change

1. Introduction

During the rocket launching process, cryogenic propellant is discharged from the tank bottom and high-temperature helium gas is generally injected into the tank to maintain the tank pressure at a sufficiently high level so as to prevent cavitation at the pump inlet. In this process, various thermodynamic phenomena may simultaneously

* Corresponding author. Tel: +86-29-82668725; Fax: +86-29-82668789
E-mail address: yzli-epe@mail.xjtu.edu.cn

1875-3892 © 2015 The Authors. Published by Elsevier B.V. This is an open access article under the CC BY-NC-ND license (http://creativecommons.org/licenses/by-nc-nd/4.0/).
Peer-review under responsibility of the organizing committee of ICEC 25-ICMC 2014
doi:10.1016/j.phpro.2015.06.047

Nomenclature

$\dot{m}$	mass transfer, kg/(m^3•s)	α	volumetric fraction
ρ	density, kg/m^3	x	mole fraction
P_{total}	total pressure, Pa	P_0	initial ullage pressure, Pa
l_{u0}	initial ullage height, m	T_{in}	inlet temperature, K
$\dot{m}_{in}$	inlet mass flux, kg/s	$\dot{V}_{out}$	outlet volume
l	distance from tank top, m	t	time, s
T_{u}	ullage temperature, K	T_{w}	wall temperature, K

occur including heat transfers between ullage, liquid and tank wall, liquid-vapor mass transfer and species transport in the multi-component ullage. A sufficient knowledge of these processes and their effects on pressurization performances are of importance for the design and optimization of a pressurization system.

Several experimental investigations have been conducted to exhibit the thermodynamic phenomena inside the cryogenic tank. Stochl et al. [1-2], Lacovic [3], Ludwig and Dreyer [4-5] applied experimental studies to obtain the pressurization performances and to evaluate the effects of various parameters on helium gas requirements. Besides, computational approaches can also be used to predict the thermal and pressurization behavior, and several computational models including the 0-D model, 1-D model and CFD model have been developed. Karimi et al. [6] and Kim et al. [7] respectively employed the 0-D model to predict the pressurization behavior for the self-pressurization or the pressurized discharge processes. Roudebush [8] developed a 1-D model to consider the ullage stratified effect for the problem of a pressurized discharge process. Masters [9] revised and extended this 1-D model to include the interfacial energy transfer in tanks of arbitrary symmetric shape and to cover the initial pressurization (ramp) period. Kwon et al [10] also developed a 1-D model to predict the helium mass requirements and an "expanding" finite volume method was applied to divide the ullage region axially. Great emphasis has been placed on the CFD investigation of tank pressurization prediction. Adnani and Jennings [11], Leuva et al. [12], Ludwig and Dreyer [5] respectively used commercial CFD software to predict the ullage pressure behavior or gas requirements during the pressurization stage. We have previously constructed a CFD model to investigate the transient thermal performance and pressurization behavior of cryogenic tanks during liquid discharge [13]. For the helium pressurization case, the propellant vapor as well as the mass transfer effect is ignored and a helium-only ullage model is applied [14].

In the present paper, an improved CFD model is introduced to investigate the thermal performance and pressurization behavior for a typical helium pressurized discharge process. Two helium pressurization cases, respectively pressurizing hydrogen tank and oxygen tank, are simulated and analyzed, and the thermal performance and pressure behavior are presented and compared. The present study will provide a more reasonable insight into the tank interior field distributions as well as the pressurization behavior.

2. CFD modeling

2.1 Physical model

The cryogenic tank in reference [13] is selected as the present research objective. Helium gas is applied as the pressurant gas, so a mixture of propellant vapor and helium gas will fill the ullage space during liquid discharge. In the present model, the species transport model is activated to consider the diffusion and mixing effect of multi-component ullage. Table 1 lists the main initial and boundary conditions for the following pressurization cases. To obtain an accurate initial field distribution, the pre-pressurization process including a ramp stage and a hold stage is also considered in the present computations. During the pre-pressurization process, warm helium gas, 100K for LH_2 tank and 300K for LO_2 tank respectively, is selected to pressurize the propellant tank from ambient state to the launching state, P_0. Other initial and boundary conditions can be seen in reference [13].

Table 1 Initial and boundary conditions for CFD simulations

Case	P_0 [MPa]	lu_0 [m]	T_{in} [K]	$\dot{m}_{in}$ [kg/s]	$\dot{V}_{out}$ [m^3/s]	t_{total} [s]	q [W/m^2]
LO_2-He	0.48	1.0	300	0.2	0.528	175	0
LH_2-He	0.48	1.0	300	0.4	0.528	175	0

2.2 Phase change model

The phase change effect is also considered in the present model. In this model, a quasi-steady thermodynamic condition is supposed and the difference between propellant fluid temperature, T, and the saturation temperature, T_{sat}, corresponding to the vapor partial pressure, P_{vapor}, is taken as the driving force of the phase change.

For $T \geq T_{sat}$ (evaporation),

$$\dot{m}_{lv} = -\dot{m}_{vl} = -C\alpha_l \rho_l \frac{|T - T_{sat}|}{T_{sat}} \tag{1}$$

For $T < T_{sat}$ (condensation),

$$\dot{m}_{vl} = -\dot{m}_{lv} = C\alpha_v \rho_v \frac{|T - T_{sat}|}{T_{sat}} \tag{2}$$

T_{sat} is calculated as follows:

$$T_{sat} = T_{sat}(P_{vapor}) \tag{3}$$

$$P_{vapor} = P_{total} \cdot x_{vapor} \tag{4}$$

3. Results and discussion

3.1 LH_2-He case

To better evaluate the predictive ability of the present CFD model, the results of the previous helium-only model and the present model are displayed in the same figures. Fig.2 displays the comparison of ullage pressure histories. It shows nearly a continuous decline of tank pressure exists in the whole discharge process. This is because the ullage-wall heat transfer rate increases with the enlargement of wall area exposed to warmer ullage and the energy left in the ullage that is providing the pressurization effect is reduced correspondingly. Moreover, the improved CFD model produces remarkably higher pressure values. The deviation of the pressures increases with time and the maximum deviation is approximate 35%. Fig.3 displays the comparison of final axial temperature profiles. It shows a warmer ullage and a colder tank wall are obtained by the present model, which may indicate that the improved model produces a weaker ullage-wall heat transfer than the previous model. Fig.4 displays the comparison of the calculated ullage-wall heat transfer rate for the two models. It can be seen clearly that ignoring the propellant vapor effect in the computation will overestimate the ullage-wall heat transfer. The average deviation of the predicting values is approximate 33.4%.

The integral mass transfer amount during the discharge is displayed in Fig.5. It shows that the phase change mode for the current LH_2-He case is evaporation. Over the whole discharge process, approximate 2kg hydrogen is transferred from liquid to vapor. Since an adiabatic heat boundary is applied to the tank wall, the energy driving mass transfer only comes from the ullage-interface heat transfer. The ratio of mass transfer amount to the

discharging liquid mass is only about 0.03%, which may indicate that the phase change effect cannot have a large influence on the liquid volumetric change.

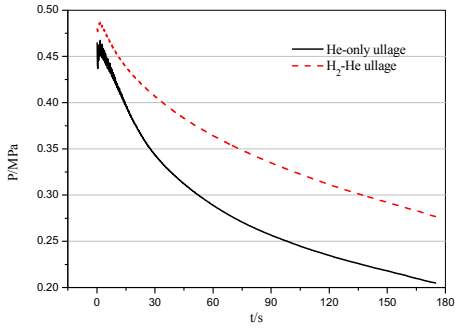

Fig.2 Comparison of pressure histories for LH_2-He case

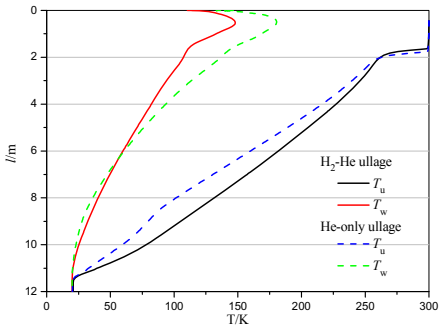

Fig.3 Comparison of final temperature profiles for LH_2-He case

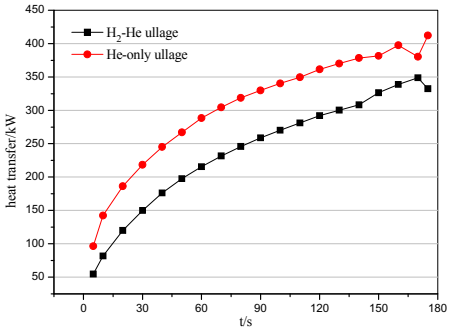

Fig.4 Comparison of fluid-wall heat transfer rate for LH_2-He case

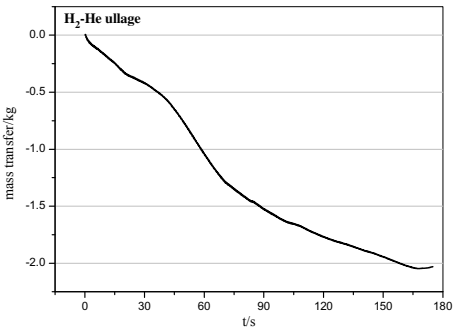

Fig.5 Mass transfer amount history for LH_2-He case

Fig.6 displays the physical field distribution contours at the end of discharge. It shows that helium gas dominates the ullage region, and propellant vapor and helium gas diffuse and mix with each other, resulting in a continuous variation of gas concentration, as shown in Fig6 (b). Moreover, it can be seen that in the lower ullage region, gas temperatures in the center are slightly lower than in the surrounding region. This is closely related to the gas concentration distribution. It shows that the hydrogen concentration in the central region is higher. Hydrogen gas has a larger specific heat, c_p, than helium, thus a higher average c_p exists in the central region. When the same energy is transferred to the multi-component ullage, the region with a larger c_p will experience a smaller temperature rise.

3.2 LO_2-He case

Fig.7 displays the comparison of pressure curves for the LO_2-He case. It also shows that higher pressure values can be obtained by the present model, and the maximum deviation is approximate 18.4%. Fig.8 displays the integral mass transfer amount during the discharge. In general, the fluid experiences a continuous vapor condensation during the first 80s and then a liquid evaporation for the remainder of discharge, which is different from that in LH_2-He case. Compared to the situation in LH_2 tank, the ullage-interface heat transfer, Q_{ui}, of the LO_2 tank is weaker because of the smaller temperature difference. The initial liquid oxygen is subcooled. Therefore, at the beginning stage of discharge, Q_{ui} is smaller than the liquid-interface heat transfer, Q_{li}, and vapor condensation occurs to balance the heat transfer difference on both sides of the interface. With the discharge process proceeding, the liquid temperature in the near-interface region rises gradually, leading to a continuous decline of Q_{li}. When Q_{ui} surpasses Q_{li}, the phase change mode turns to liquid evaporation.

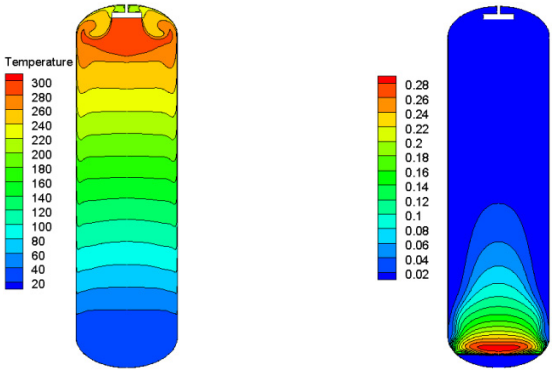

(a) temperature (b) H_2 mass fraction

Fig.6 Physical field distribution at the end of discharge for LH_2-He case

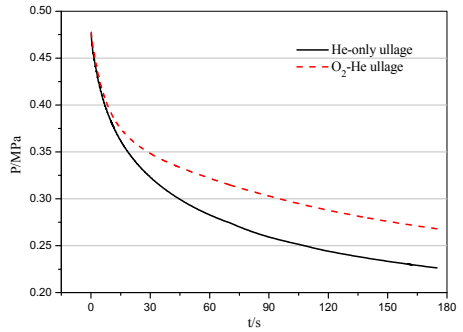

Fig.7 Comparison of pressure altering curves for LO_2-He case

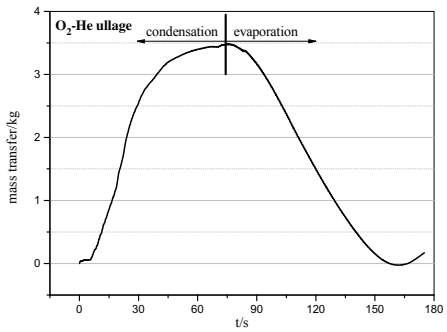

Fig.8 Mass transfer amount history for LO_2-He case

Fig.9 illustrates the physical field distribution contours for the LO2-He case. It shows that a significant radial temperature distribution exists in the lower ullage region. For the radial temperature distribution, the temperature at the central region is higher than that in the surrounding region. This phenomenon can also be attributed to the gas concentration distribution. In the lower ullage region, oxygen gas has an obvious radial concentration distribution and the central oxygen concentration is higher. Also, oxygen gas has a lower c_p than helium. When equivalent heat is transferred to the multi-component ullage, the central region with much oxygen will experience a large temperature rise than that in surrounding region.

4. Conclusions

Several main conclusions may be made as follows:

(1) Compared to the helium-only ullage model, the present model produces a weaker fluid-wall heat transfer rate, and further results in a higher ullage temperature as well as the pressurization behavior.

(2) The multi-component ullage will affect the properties variations within the ullage, leading to an observable radial temperature distribution, especially for the liquid oxygen tank.

(3) The phase change mode of the LH_2-He case is liquid evaporation, while the LO_2-He case experiences first the vapor condensation and then the liquid evaporation process during the whole discharge. On the whole, the phase change effect is very small and has a slight influence on the pressurization performance.

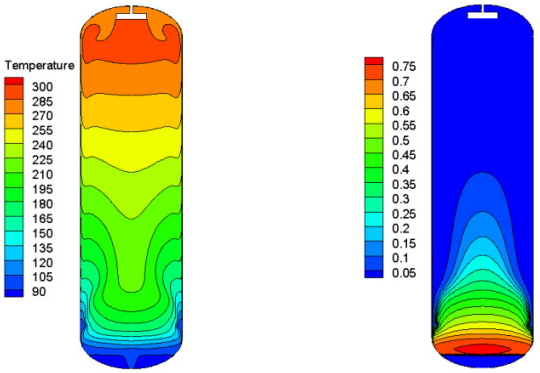

(a) temperature (b) O_2 mass fraction

Fig.9 Physical field distribution at the end of discharge for LO_2-He case

Acknowledgements

This work was financially supported by the China Postdoctoral Science Foundation (2014M550487), the National Natural Science Foundation of China (51376142) and the Research fund of State Key Laboratory of Technologies in Space Cryogenic Propellants (SKLTSCP1311).

References

[1] Stochl RJ, Maloy JE, Masters PA, et al. Gaseous-helium requirements for the discharge of liquid hydrogen from a 1.52-meter-(5-ft-) diameter spherical tank. *NASA TN D-5621*; 1970,

[2] Stochl RJ, Maloy JE, Masters PA, et al. Gaseous-helium requirements for the discharge of liquid hydrogen from a 3.96-meter-(13-ft-) diameter spherical tank. *NASA TN D-7019*; 1970.

[3] Lacovic RF. Comparison of experimental and calculated helium requirements for pressurization of a centaur liquid oxygen tank. *NASA TM X-2013*; 1970.

[4] Ludwig C, Dreyer ME. Analyses of cryogenic propellant tank pressurization based upon ground experiments. *AIAA 2012-5199*; 2012.

[5] Ludwig C, Dreyer ME. Investigation on thermodynamic phenomena of the active-pressurization process of cryogenic propellant tank. *Cryogenics* 2014; DOI：10.1016/j.cryogenics.2014.05.005.

[6] Karimi H, Nassirharand A, Mohseni M. Modeling and simulation of a class of liquid propellant engine pressurization systems. *Acta Astronaut* 2010; 66:539-49.

[7] Kim KH, Ko HJ, Kim K, et al. Transient thermal analysis of a cryogenic oxidizer tank in the liquid rocket propulsion system during the prelaunch helium gas pressurization. *J Eng Thermophys-Rus* 2012; 21(1): 1-15.

[8] Roudebush WH. An analysis of the problem of tank pressurization during outflow. *NASA TN D-2585*; 1965.

[9] Masters PA. Computer programs for pressurization (RAMP) and pressurized expulsion from a cryogenic liquid propellant tank. *NASA TN D-7504;* 1974.

[10] Kwon O, Kim B, Kil G, et al. Modeling the prediction of helium mass requirement for propellant tank pressurization. *J Spacecraft rockets* 2012; 49(6): 1150-8.

[11] Adnani P, Jennings RW. Pressurization analysis of cryogenic propulsion systems. *AIAA 2000-3788*; 2000.

[12] Leuva D, Gangadharan S, Wilson P, et al. A CFD study of cryogenic LH2 tank ullage pressurization. *AIAA 2012-1888*; 2012.

[13] Wang L, Li YZ, Li C, et al. CFD investigation of thermal and pressurization performance in LH2 tank during discharge. *Cryogenics* 2013; 57:63-73.

[14] Wang L, Li YZ, Zhao ZX, et al. Transient thermal and pressurization performance of LO2 tank during helium pressurization combined with outside aerodynamic heating. *Int J Heat Mass Tran 2013*; 62: 263-71.